An epigenetic component of hematopoietic stem cell aging amenable to reprogramming into a young state.

Wahlestedt, Martin; Norddahl, Gudmundur; Sten, Gerd; Ugale, Amol; Micha Frisk, Mary-Ann; Mattsson, Ragnar; Deierborg, Tomas; Sigvardsson, Mikael; Bryder, David

Published in:
Blood

DOI:
10.1182/blood-2012-11-469080

2013

TITLE PAGE

An Epigenetic Component of Hematopoietic Stem Cell Aging Amenable to Reprogramming Into a Young State

Martin Wahlestedt[1], Gudmundur L Norddahl[1], Gerd Sten[1], Amol Ugale[1], Mary-Ann Micha Frisk[2], Ragnar Mattsson[2], Tomas Deierborg[3], Mikael Sigvardsson[4] and David Bryder[1].

[1] Lund University, Medical Faculty, Institution for Experimental Medical Science, Immunology Section, Tornavägen 10, BMC D14, 221 84, Lund, Sweden

[2] Lund University, Medical Faculty, Institution for Experimental Medical Science, Transgenic Core Facility, Tornavägen 10, BMC C13, 221 84, Lund, Sweden

[3] Lund University, Medical Faculty, Institution for Experimental Medical Science, Neuronal Survival Unit, Tornavägen 10, BMC B11, 221 84, Lund, Sweden

[4] Linköping University, Institution of Clinical and Experimental Medicine, Sandbäcksgatan 7, 581 83, Linköping, Sweden

Running title: Epigenetic Reversal of HSC aging
Text word count: 4000, Abstract word count: 172
Number of figures and tables: 4
Number of references: 34
Corresponding author: David.Bryder@med.lu.se, Phone number: +46-46-2223951, Fax number +46-46-222 42 18

KEY POINTS

1) **Hematopoietic stem cell aging associate with stable transcriptional alterations that persist through transplantation.**

2) **Somatic cell reprogramming of aged hematopoietic stem and progenitor cells reverses functional defects associated with hematopoietic aging.**

ABSTRACT

Aging of hematopoietic stem cells (HSCs) leads to several functional changes, including alterations affecting self-renewal and differentiation. While it is well established that many of the age-induced changes are intrinsic to HSCs, less is known about the stability of this state. Here, we entertained the hypothesis that HSC aging is driven by the acquisition of permanent genetic mutations. To examine this issue at a functional level in vivo, we applied induced pluripotent stem (iPS) cell reprogramming of aged hematopoietic progenitors and allowed the resulting aged-derived iPS cells to reform hematopoiesis via blastocyst complementation. Next, we functionally characterized iPS-derived HSCs in primary chimeras and following the transplantation of 're-differentiated' HSCs into new hosts; the gold standard to assess HSC function. Our data demonstrate remarkably similar functional properties of iPS-derived and endogenous blastocyst-derived HSCs, despite the extensive chronological and proliferative age of the former. Our results therefore favor a model in which an underlying, but reversible, epigenetic component is a hallmark of HSC aging rather than being driven by an increased DNA mutation burden.

INTRODUCTION

Many of the pathologies that could benefit from regenerative stem cell based therapies are age-associated[1]. An evident example is represented by bone marrow (BM) transplantation, a therapeutic modality that relies on the regenerative capacity of hematopoietic stem cells (HSCs) and where graft age is one of the most significant negative parameters for successful outcome[2]. One key mechanism proposed to underlie HSC aging involves the acquisition of permanent genetic changes such as accumulation of DNA damage and/or telomere attrition[3]. Yet, while there is a potential role for DNA damage in HSC aging, it is currently unclear if accumulation of DNA damage could explain all or even a part of the distinct transcriptional changes that associate with HSC aging and that ultimately underlie their altered function [4-7].

For the purpose of regenerative medicine, alterations in the underlying genomic DNA sequence would be problematic to correct efficiently. By contrast, it might be more conceivable to alter the regulation of the transcriptome of a stem cell population, assuming permanent genomic damage does not underlie and dictate the transcriptional changes. One conceptual example is represented by induced pluripotent stem cells (iPS). iPS cells, created by transcription factor-mediated reprogramming of somatic cells[8], progressively gain particular epigenetic features during the reprogramming process while simultaneously loosing those of the somatic starting cell[9,10], to finally reach a relatively stable embryonic stem cell (ES)-like state[11].

Here, to explore the stability and potential reversibility of hematopoietic progenitor cell aging, we generated iPS cells from aged hematopoietic stem and progenitor cells (HSPCs). Next, we used these iPS cells to complement blastocysts. IPS-derived HSCs in chimeric mice were evaluated for several parameters normally altered with age, including their telomere length, reconstitution ability, lineage competence and production of naïve T cells. Our data suggest that a dominant feature of chronological HSC aging is an epigenetic “drift”, which can be reversed by epigenetic reprogramming.

MATERIALS AND METHODS

Mice

All mice were on a C57BL/6 background with the congenic marker combinations CD45.1, CD45.2 or F1CD45.1 x CD45.2. Animals were housed at animal facilities at Lund University. The Transgenic Core Facility at Lund University performed blastocyst injections. All animal experiments were performed with consent from a local ethical committee.

Retrovirus production

Retroviral vectors (pMXs-*Oct3/4*-IP, pMXs-*Sox2*-IP, pMXs-*Klf4*, pMXs-*c-Myc*-IP) were acquired from Addgene (Cambridge, MA) and were generously deposited by Shinya Yamanaka. pMX-*GFP* was obtained from Cell Biolabs (San Diego, CA). Replication incompetent viruses were produced by transfecting the vectors into Plat-E packaging cells (Cell Biolabs, San Diego, CA) using Lipofectamine 2000 (Invitrogen, Carlsbad, CA). Supernatants were harvested 48h post transfection and titered using the Retro-X qRT-PCR Titration Kit (Clontech, France) and FACS (for pMX-*GFP*). Viruses used in experiments had titers ranging from 4×10^6 to 4×10^8 viral particles/ml.

Hematopoietic stem and progenitor isolation

For iPS generation, mouse bone marrow was depleted of mature cells using a cocktail of biotinylated antibodies (B220, CD4, CD8a, CD11b, Gr-1, Ly6c, Ter119) together with anti-biotin MACS beads (Miltenyi Biotech, Germany), before being further enriched for hematopoietic stem and progenitor cells (HSPCs) by magnetic enrichment of CD117 positive cells (Miltenyi Biotech, Germany). For HSPCs isolation and analysis, lineage-depleted samples were stained with Streptavidin conjugated to QD605 (Invitrogen, Carlsbad, CA) and antibodies recognizing c-Kit, Sca-1, CD48, CD105, CD150, CD45.1 and CD45.2, and sorted on a FACS Aria. Propidium iodide (Invitrogen, Carlsbad, CA) was used to exclude dead cells.

iPS generation from hematopoietic stem and progenitor cells

For prestimulation of primary cells prior to and during transduction, cells were cultured in OptiMEM (Invitrogen, Carlsbad, CA) supplemented with 10% Fetal Calf Serum (FCS), Penicillin/Streptomycin (Invitrogen, Carlsbad, CA), 50 ng/ml SCF, 5 ng/ml IL3 (Peprotech Inc.) and 5 U/ml EPO (Janssen-Cilag, Bersee, Belgium). Both candidate and established iPS cells were cultured under standard ES cell conditions; grown on irradiated mouse embryonic fibroblasts in DMEM (Invitrogen, Carlsbad, CA) containing 15% FCS, Penicillin/Streptomycin (Invitrogen, Carlsbad, CA), 1 mM Sodium pyruvate (Invitrogen, Carlsbad, CA), 0.1 mM β-mercaptoethanol (Invitrogen, Carlsbad, CA), 1x MEM NEAA (Invitrogen, Carlsbad, CA) and 10^3 U/ml LIF (Millipore, Billerica, MA).

To generate iPS lines, 50,000 $Lin^-c\text{-}Kit^+$ cells were transduced for 2 days using Retronectin (Takara Bio Inc., France) coated plates preincubated with retroviruses and thereafter transferred to ES cell culture conditions. The cells were cultured for 14 days with daily media changes. On day 14, 25 candidate iPS cells were sorted into individual wells of a 96-well plate in ES cell culture conditions based on their negativity for GFP, as iPS induction coincides with efficient silencing of retroviral long terminal repeat regions[8] and CD45, a pan-hematopoietic marker lost during iPS conversion, and by being SSEA-1 and Epcam positive.

Characterization of iPS clones.

iPS lines were assayed for viral vector integration by PCR using one primer specific for each vector's coding sequence and a common primer directed against the vector backbones. Chimeric mice were genotyped with a similar strategy. PCR reactions were run using Taq polymerase (Takara Bio Inc., France) with initial incubation at 94°C for 2min followed by 35 cycles of 30 sec at 94°C, 30 sec at 60°C and 30 sec at 72°C. *In vitro* differentiation capacity was investigated by embryoid body formation by cultivating 250 ES or iPS cells in 20ul hanging droplets for 48h in IMDM (Invitrogen, Carlsbad, CA) supplemented with 20% FCS, Penicillin/Streptomycin (Invitrogen, Carlsbad, CA), 1 mM Sodium pyruvate (Invitrogen, Carlsbad, CA), 0.1 mM β-mercaptoethanol (Invitrogen, Carlsbad, CA) and GlutaMAX (Invitrogen, Carlsbad,

CA). Thereafter, cells were pooled and cultured in petri dishes for 12-14 days before analysis. To verify iPS chimerism in adult mice, hippocampal brain sections were used to detect Y chromosome (from iPS cells) by starFISH fluorescence In Situ hybridization protocol (Cambio Ltd, Cambridge, UK).

Bone marrow transfer and peripheral blood analysis

For bone marrow reconstitution experiments, young CD45.2 mice were lethally irradiated with 800 rad 3-4h prior to transplantation. Whole bone marrow (2-5 x 10^6 cells) or purified HSCs (200 or 1,500 cells) together with 300,000 unfractionated BM support cells were injected into the tail-vein of recipient animals in a volume of 500 ul. Long-term contribution to the different peripheral blood cell lineages was followed over 16 weeks to assess long-term contribution of the transplanted HSCs. The analysis of the peripheral blood was done as described[12]. Samples were analyzed on an LSRII (Becton Dickinson, Franklin Lakes, NJ). The competitive ability / transplanted HSC was measured as X = ((Y*Z) / (1-Z)) / N, where X is the competitive ability/transplanted HSC, Y the estimated number of transplanted competitor HSCs (based on the fact that HSCs exist at a frequency of roughly 1/10,000 BM cells), Z the long-term myeloid chimerism and N the actual, or estimated, number of test HSCs transplanted.

Measurement of T cell excision circles

T cell receptor excision circles (TRECs) were measured in sorted CD4+/CD8+ splenic T cells by adapting a previously described protocol[13]. Briefly, the sorted cells were lysed using Proteinase K (Roche, Mannheim, Germany) and assayed for relative TREC content using a SYBR green-based qPCR approach where the cycle threshold value of a primer pair directed against a TREC was normalized against that of the single-copy gene Myt-1. To measure the naïve T cell competence of HSCs in BM transfer experiments, the chimerism of the splenic CD4+/CD8+ compartment was divided by the actual, or estimated, number of transplanted HSCs and multiplied by the relative TREC incidence acquired by qPCR.

Telomere length measurement

To estimate telomere lengths in individual cells, single-cells were isolated using FACS and assayed as previously described[14-16].

Affymetrix gene expression analysis

RNA was extracted from 10,000 sorted HSCs ($Lin^-Sca1^+c\text{-}Kit^+CD48^-CD150^+$) isolated from young or aged mice, or from recipients of young and old bone marrow cells, where they in addition were selected for appropriate CD45 isoform expression, using the RNeasy-micro mRNA purification kit (QIAGEN, Hilden, Germany) as previously described[12]. Following a two-round amplification protocol, biotin labeling and hybridization to Affymetrix 430.2 gene expression arrays, probe level expression values were extracted using RMA[17] and analysis performed using the dChip software[18] following filtering of probes with a lower expression than 100 in either experimental group. To identify differentially expressed genes with age (Figure 1A), genes with a >1.5-fold difference in expression with a confidence interval of >90% were extracted. The microarray data used in this study can be found in the Gene Expression Omnibus (http://www.ncbi.nlm.nih.gov/geo/) under accession numbers GSE44923 and GSE27686 (steady-state HSCs), GSE44923 (transplanted HSCs), GSE44923 (YoungBiPS, AgedBiPS and ES cells), GSE6503 (comparative dataset 1), GSE4332 (comparative dataset 2).

qPCR Primers used for SYBR Green mRNA expression analysis

Oct3/4 5’-TTCTAGCTCCTTCTGCAGGG -3’ (Fw)

5’-AGAGGGAACCTCCTCTGAGC-3’ (Rev)

Sox2 5’-CTCTGCACATGAAGGAGCAC-3’ (Fw)

5’-CCGGGAAGCGTGTACTTATC-3’ (Rev)

Klf4 5’-CAGTCGTAAGGTTTCTCGCC-3’ (Fw)

5’-GCCACCCACACTTGTGACTA-3’ (Rev)

c-Myc 5’-ACGGAGTCGTAGTCGAGGTC-3’ (Fw)

5’-AGAGCTCCTCGAGCTGTTTG-3’ (Rev)

Nanog 5’-ATGCCTGCAGTTTTTCATCC-3’ (Fw)

5’-GAGGCAGGTCTTCAGAGGAA-3’ (Rev)

β-actin 5’-CCACAGCTGAGAGGCAAATC-3’ (Fw)

5’-CTTCTCCAGGGAGGAAGAGG-3’ (Rev)

qPCR Primers used for genomic DNA analysis

Oct3/4 5’-CAGTCCAACCTGAGGTCCAC-3’ (Rev)

Sox2 5’-CCGGGACCATACCATGAA-3’ (Rev)

Klf4 5’-TCCTCACGCCAACGGTTAGT-3’ (Rev)

c-Myc 5’-AGGGCTGTACGGAGTCGTAG-3’ (Rev)

Universal forward primer (viral backbone):

5’ GACGGCATCGCAGCTTGGATACAC-3’

sjTREC 5’-CCAAGCTGACGGCAGGTTT-3’ (Fw)

5’-AGCATGGCAAGCAGCACC-3’ (Rev)

Myt-1 5’-TGCCACCGCTGCTAATGAG -3’ (Fw)

5’-TGCGAACTCCTAAGCCAGCTA-3’ (Rev)

Telomeric repeats:

5’-CGGTTTGTTTGGGTTTGGGTTTGGGTTTGGGTTTGGGTT-3’ (Fw)

5’-GGCTTGCCTTACCCTTACCCTTACCCTTACCCTTACCCT-3’ (Rev)

Statistical analysis

Genome-wide gene expression microarray data were analyzed using dChip and GSEA, according to manufacturer’s instructions. For fold-over-odds calculations, we

applied a binomial probability calculation (Poisson distribution approximation). Otherwise, significance values were calculated by Student's two-tailed t-test.

RESULTS

Genome-wide expression profiling reveals that an aging hematopoietic stem cell signature is maintained following transplantation

It is well established that aging imposes several functional shortcomings on HSCs, including pronounced shifts in the types of mature effector cells produced and alterations in self-renewal[19]. Most existing data argue that these features are autonomous to HSCs since arising phenotypes are visualized when transplanting aged HSCs into young hosts, but not vice versa[4]. However, one concern with HSC transplantation experiments is that they tend to evaluate HSC function based on retrospective analysis of the produced progeny rather than directly at the level of HSCs. To begin to approach this issue, we transplanted young lethally irradiated mice with stem and progenitor cell-enriched bone marrow cells from young and old donors. 4 months post-transplant, we isolated highly purified linage negative, Sca-1+, ckit+, CD48- and CD150+ HSCs from these reconstituted animals, and performed genome-wide expression analyses using Affymetrix 430.2 microarrays ("Transplanted HSCs"; 2 biological arrays/condition). We reasoned that this strategy would provide a mean to expose relatively permanent intrinsic gene expression changes, separate from those that associate strictly with cell division, as transplantation enforces vigorous cell cycling of the otherwise quiescent HSCs[20]. By stringent analysis criteria, these experiments revealed differential expression of 573 probe sets (332 with lower and 241 with higher expression in HSCs derived from aged donors; Table S1). Next, we conducted similar analyses on HSCs from young and aged "steady-state" donors (6 biological replicates for each condition). These experiments revealed 490 probe sets with differential expression in the steady-state situation (Table S1), with the majority being upregulated in aged HSCs (342 probe sets). The gene lists obtained from our two lines of experiments were next intersected to investigate a potential overlap. This revealed a highly significant

correlation for both the "Young-associated" (Figure 1A, odds-ratio: 5.1; p=0.000002) and "Aging-associated" (Figure 1B, odds-ratio: 10.7; p<0.000001) probe sets. In an alternative analysis, we implemented Gene Set Enrichment Analysis (GSEA)[21]. This independent approach confirmed a highly significant association of the steady-state young and aged HSC profiles to those obtained from young and aged HSCs subjected to transplantation (p<0.001 for both up- and down-regulated genes, Figure S1). A large proportion of these stably differentially expressed genes were also differentially expressed in two independently generated datasets[4,5] of steady-state young and aged HSCs (Figure S2). These data establish that a core set of transcriptional alterations associate with HSC aging. These, in turn, persist through the multiple rounds of cell divisions that associate with HSC transplantation, and can therefore be regarded as relatively stable.

Establishment of iPS lines from young and aged hematopoietic progenitor cells

To generate iPS cells from hematopoietic progenitor cells, Lin-c-Kit+CD45.1+ HSPCs from young or aged mice were isolated and infected for two consecutive days with retroviruses carrying *GFP*, *Oct3/4*, *Klf4*, *c-Myc* and *Sox2*. Thereafter, the cells were transferred to embryonic stem (ES) cell culture conditions. After 4-7 days of culture, we began to observe a vast growth of cells, with the emergence of ES-like colonies from day 14 and onwards. However, the vigorous proliferation of other cells persisted in these cultures, complicating the isolation of emerging iPS colonies. To circumvent this problem, we isolated candidate iPS cells from other cells by FACS using antibodies against EpCAM (CD326)[22] and SSEA-1 (Figure 2A). This strategy enabled effective removal of other proliferating non-iPS cells (Figure 2B and data not shown). Two iPS lines derived from young HSPCs (Young Blood induced Pluripotent Stem cells; "Young BiPS") and two lines derived from aged HSPCs ("Aged BiPS") were selected for further experimentation.

In initial analyses, we confirmed expression of pluripotency factors and induction of Nanog expression by qRT-PCR in the newly generated iPS lines from both young and old mice (Figure 2C). To obtain a wider view of their transcriptional signatures, we performed gene expression analyses of established iPS lines using

microarrays. For comparative purposes, we also included samples from three different C57BL/6 ES cell lines. Regardless of young or aged origin, these analyses revealed highly similar expression patterns of BiPS cells to ES cells (Figure 2D). By contrast, and as expected, large differences in expression patterns was observed when comparing iPS or ES cell lines to HSCs (Figure 2D).

To functionally characterize the generated iPS lines, we first investigated their potential to produce contracting cardiomyocytes *in vitro* (Movie S1). These experiments verified their potential to produce cells of an alternative lineage, but of the same germ layer (mesoderm) as the original somatic donor cells. To further investigate their lineage potential, we performed a series of blastocyst injections (Table S2). First, to investigate the potential of BiPS cells to produce a cell lineage with an alternative (ectodermal) germ layer origin than the starting blood cells, we investigated neurons in the hippocampus using Y-chromosome detection in brain sections from a female mouse chimeric with male aged BiPS cells. These analyses confirmed the presence of robust chimeric contribution to the neural lineage (Figure 2E). Finally, we set up breeding with a male aged BiPS chimeric male with a wild-type C57BL/6 female, and screened two litters of offspring for germline transmission. Of 17 pups screened, we obtained one mouse with its blood system composing entirely of F1 CD45.1 x CD45.2 cells (Figure 2F), with CD45.1 representing a marker of BiPS cells (see below), thereby establishing totipotency of the generated BiPS cells.

Telomere length maintenance of steady state aged and aged BiPS-derived hematopoietic stem cells

Somatic stem cell pools, including HSCs, are needed for the lifetime of an organism[19]. However, increasing numbers of cell divisions could potentially lead to shortening of telomeres, a mechanism previously proposed to regulate stem cell behavior[23]. We reasoned that this aspect could be particularly relevant in the context of our aged BiPS cells, given their proliferative history both as a consequence of their chronological age and because of the substantial proliferation induced in these cells upon the iPS induction and maintenance. To approach this issue, we examined the telomere length in individual steady-state young (n = 251) and aged (n =246) HSCs.

These data established that aged HSCs harbored approximately 11% shorter telomeres in comparison to their young counterparts ($p<0.0234$, Figure 3A), which represents the baseline effect of aging on the telomere length of HSCs.

Although a few previous studies have reported a significant elongation of telomeres in established iPS cell lines compared to the telomere length of the somatic donor cell type[24,25], it has remained unclear whether telomere length is appropriately maintained following re-differentiation of iPS cells. Furthermore, it remained a formal possibility that the somatic cell type itself might influence on the telomere length dynamics associated with iPS formation and maintenance. This was relevant to our work, as we used hematopoietic cells, while most previous studies on iPS cells have used fibroblasts as somatic donor cells. When investigating aged BiPS derived HSCs in the primary chimeric setting (which due to cell availability was restricted to the aged BiPS2 clone), we found a striking (2-fold, $p<0.0001$) elongation of telomeres compared to the blastocyst control HSCs (Figure 3B). Next, we conducted similar experiments on aged BiPS-derived HSCs following transplantation. These experiments demonstrated that aged BiPS maintained their approximately 2-fold elongated telomeres ($p<0.0001$ for both Aged BiPS1 and Aged BiPS2), despite the exposure of these cells to severe hematopoietic stress/proliferation (Figure 3C). Finally, we investigated the telomere length of HSCs derived from a germline offspring mouse (see Figure 2F). From this mouse, we could observe a significant reduction in telomere length as compared to the telomere length of HSCs from the primary chimera (parent), although telomere length still remained significantly longer in such offspring (approximately 31% longer compared to that of the somatic starting cells, $p<0.0001$) (Figure 3D). Taken together, these experiments demonstrate that iPS formation from HSPCs associates with elongation of telomeres in a similar manner as previously described for iPS cells with a fibroblast origin[24].

Reprogramming of aged hematopoietic progenitors into totipotency alleviates the functional alterations that associate with chronological hematopoietic aging

As a last and main aim of our work, we set out to functionally characterize the hematopoietic differentiation capacity of BiPS from aged HSPCs. Despite extensive

research, the exact cues guiding *in vitro* differentiation of ES/iPS cells into adult-type HSCs have not yet been established. Therefore, we evaluated the hematopoietic differentiation potential of young BiPS and aged BiPS cells in chimeric mice generated via blastocyst injections (Table S2). Because we had a specific interest in the hematopoietic system, we had initially devised our experiments such that we could evaluate the BiPS derived contribution using the congenic CD45.1 (expressed on BiPS cells) and CD45.2 (blastocyst derived cells) markers. As CD45 is expressed on all nucleated blood cells, this made it possible to detail hematopoiesis derived from young BiPS and aged BiPS in chimeric mice in a direct manner.

As lineage skewing is a dominant feature of HSC aging, we first evaluated the lineage distribution of BiPS derived cells in the primary chimeric mice[26-29]. These analyses revealed that the hematopoietic lineage distributions of iPS-derived cells, regardless of origin, were remarkably similar to those of the endogenous blastocyst origin (Figure 4A). Another hallmark of HSC aging is a dramatic increase in numbers of phenotypically defined HSCs[4,5,27,28]. We therefore evaluated this aspect in mice chimeric with aged BiPS cells, but failed to observe any differences when comparing to the blastocyst-derived HSCs (Figure 4B). By contrast, and in agreement with previous data[4,5,27,28], aged steady-state mice displayed dramatically elevated frequencies of HSCs (12.9-fold, $p<0.0001$; Figure 4B).

Next, we explored the capacity of aged BiPS cells to regenerate a hematopoietic system in a competitive transfer setting. To this end, we transplanted BM mononuclear cells from primary aged BiPS chimeric mice into lethally irradiated CD45.2 recipient hosts (2-5 x 10^6 cells/mouse). 16 weeks after transplantation, we evaluated the aged BiPS and blastocyst derived hematopoiesis in the peripheral blood of these hosts. These experiments revealed the aged BiPS reconstitution to be of similar magnitude and quality when compared to the reconstitution patterns obtained from young HSCs in steady state (Figure 4C and 4D), as well as to the reconstitution pattern observed from the blastocyst control (Figure 4D). This was in sharp contrast to chronologically aged HSCs, which were characterized by a dramatic reduction in repopulation capacity (23.8-fold, $p<0.0001$) (Figure 4C). Finally, we performed more detailed investigations to explore the intrinsic ability of aged BiPS-

derived HSCs to generate naïve T cells. We were particularly interested in this aspect as this parameter is normally difficult to probe in steady-state aged mice due to the thymic atrophy that accompanies aging. To this end, we estimated the frequencies of T cells containing T-cell receptor excision circles (TRECs), a molecular marker of recent thymic emigrants[13], per transplanted HSC. These analyses revealed that steady-state aged HSCs have a strongly reduced T cell potential when compared to their young counterparts (38.4-fold reduction, p=0.005, Figure 4E). By contrast, aged BiPS derived HSCs generated naïve T cells at similar levels as both young HSCs and the endogenous blastocyst control-derived HSCs (Figure 4E).

ISCUSSION

Many parameters act together and complicate both the study and generalizations that can be made about the aging of multicellular organisms. These include not only the highly varying onset in both time and degree whereby aging affects different organs and tissues, but also its pleiotropic outcomes. Such considerations aside, one common feature of aging involves what seems as an inevitable loss of overall fitness. At a cellular level, this could result in either the generation of functionally defective cells, a reduced ability in the generation of appropriate cells, or a combination of both scenarios. The recognition that most organs and tissues are maintained by primitive self-renewing stem cells, whose sole function is to provide organisms with appropriate cellular offspring for a lifetime, has in recent years fuelled the emergence of theories of stem cell origins to the aging process[3,19]. The blood system is particularly amenable to study the autonomous aspects of these processes because of its extensively well-established character and the ability to regenerate an entire blood system from HSCs via transplantation.

An initial striking observation made in these studies was the dramatic elongation of telomeres that associated with the reprogramming process. These telomeres were appropriately maintained during the transition of iPS cells to differentiated progeny, and required germline dilution for substantial shortening, which agree with recent data showing that the combined telomere lengths of the

parents determine telomere lengths of offspring[30]. However, while telomere extension may be a necessity for the generation of functional iPS cells, the long telomeres of C57BL/6 mice[14] combined with the fact that chronologically aged HSCs show only modest telomere shortenings, argue perhaps against telomere attrition as the primary driver of murine HSC aging.

We interpret our results on the "young-like" functional capacity of aged-derived BiPS cells to support a view in which reversible epigenetic (and transcriptional) alterations are central for the development and/or maintenance of the phenotypes associated with HSC aging. While a few reports have previously suggested that iPS cells themselves can associate with varying degrees of molecular "resemblance", or "memory" of its somatic donor origin[31,32], we could find little evidence for an epigenetic memory with functional consequences in the BiPS lines studied here. Some data argue that this central question perhaps can be explained from the perspective of an incomplete reprogramming process[33]. In an alternative interpretation, it might be envisioned that the strategy used in our work could favor selection of a subset of HSPCs unaffected by age and/or DNA damage. While we formally cannot rule out this possibility, we however consider it less likely. This is foremost based on the similarities in efficiencies of iPS formation of young and aged HSPCs (unpublished observations), and the very strong dominance of myeloid-biased HSCs in the aging setting[4]. It might also be conceivable that aging HSPCs have acquired mutations that by themselves result in altered epigenetic features. An extension of this view would be that initial causative mutations would be compensated for during the iPS process and thus redundant for subsequent re-differentiation. Our experiments did not address this issue directly, but we did find that young BiPS, aged BiPS and ES cells had remarkably similar genome-wide expression profiles and thus showed no evidence of transcriptional compensation.

Previously, sequencing of murine iPS lines revealed a mutational spectra correlating distinctly to that observed in the somatic cell donor cells[34]. Based on such data, it can be anticipated that if murine HSPC aging do associate with an increase DNA mutation frequency, similar to the aging of human healthy HSPC[35], then aged BiPS lines should have significantly more DNA mutations. However, even if this could

be established, its consequence would require extensive sequencing combined with loss and/or gain of function studies; a line of experiments beyond the scope of the work presented here.

We interpret our data to show that the epigenetic reset coinciding with iPS induction has immediate functional benefits for subsequent differentiation. This should be the result of normalized regulation of certain defined loci dysregulated with age, and thus a careful evaluation of the epigenetic properties of aged HSPCs might provide both candidate genes and more general regulators. For instance, the key epigenetic regulator *Ezh2* is down regulated in aged HSCs[36]. Although we previously found little evidence of epigenetic changes at the *p16INK4a* locus in aged HSCs[36], a well-established *Ezh2* target loci in other cells[37], the broad and potent roles of *Ezh2* might well underlie other epigenetic alterations governing the HSC aging process[38].

In conclusion, our experiments demonstrate that reprogrammed aged HSPCs have functional differentiation potential similar to those of vastly younger cells. Whether the aging state can be subjected to reversal in a more physiologic or less invasive setting, and not merely in a highly artificial reprogramming scenario, remains a key outstanding question.

ACKNOWLEDGEMENTS

This work was generously supported by project grants to DB from the Swedish Cancer Society, the Swedish Medical Research Council (project grants and consortia grants Hemato-Linné and Stemtherapy), the Swedish Pediatric Leukemia Foundation, Ingabritt och Arne Lundbergs Forskningsstiftelse and an AFA grant for research on regenerative medicine.

AUTHORSHIP

Contribution: D.B. and M.W. planned the study; M.W., G.L.N, G.S. and A.U. performed most experiments; M.M-F. and R.M. undertook the blastocyst injections; T.D. performed the FISH experiments; M.S. helped with microarray hybridizations. M.W., G.L.N. and D.B analyzed the data and wrote the manuscript.

Conflict-of-interest disclosure: The authors declare no conflicts of interest.

Correspondence: David Bryder, Immunology section, Institution for Experimental Medical Science, BMC D14, 221 84, Lund, Sweden. Email: David.Bryder@med.lu.se.

REFERENCES

1. Gurtner GC, Callaghan MJ, Longaker MT. Progress and potential for regenerative medicine. *Annu Rev Med*. 2007;58:299-312.
2. Kollman C, Howe CW, Anasetti C, et al. Donor characteristics as risk factors in recipients after transplantation of bone marrow from unrelated donors: the effect of donor age. *Blood*. 2001;98(7):2043-2051.
3. Sharpless NE, DePinho RA. How stem cells age and why this makes us grow old. *Nat Rev Mol Cell Biol*. 2007;8(9):703-713.
4. Rossi DJ, Bryder D, Zahn JM, et al. Cell intrinsic alterations underlie hematopoietic stem cell aging. *Proceedings of the National Academy of Sciences of the United States of America*. 2005;102(26):9194-9199.
5. Chambers SM, Shaw CA, Gatza C, Fisk CJ, Donehower LA, Goodell MA. Aging hematopoietic stem cells decline in function and exhibit epigenetic dysregulation. *PLoS biology*. 2007;5(8):e201.
6. Noda S, Ichikawa H, Miyoshi H. Hematopoietic stem cell aging is associated with functional decline and delayed cell cycle progression. *Biochem Biophys Res Commun*. 2009;383(2):210-215.
7. Pang WW, Price EA, Sahoo D, et al. Human bone marrow hematopoietic stem cells are increased in frequency and myeloid-biased with age. *Proc Natl Acad Sci U S A*. 2011;108(50):20012-20017.
8. Takahashi K, Yamanaka S. Induction of pluripotent stem cells from mouse embryonic and adult fibroblast cultures by defined factors. *Cell*. 2006;126(4):663-676.
9. Hawkins RD, Hon GC, Lee LK, et al. Distinct epigenomic landscapes of pluripotent and lineage-committed human cells. *Cell stem cell*. 2010;6(5):479-491.
10. Brambrink T, Foreman R, Welstead GG, et al. Sequential expression of pluripotency markers during direct reprogramming of mouse somatic cells. *Cell Stem Cell*. 2008;2(2):151-159.
11. Maherali N, Sridharan R, Xie W, et al. Directly reprogrammed fibroblasts show global epigenetic remodeling and widespread tissue contribution. *Cell stem cell*. 2007;1(1):55-70.
12. Norddahl GL, Pronk CJ, Wahlestedt M, et al. Accumulating mitochondrial DNA mutations drive premature hematopoietic aging phenotypes distinct from physiological stem cell aging. *Cell stem cell*. 2011;8(5):499-510.
13. Sempowski GD, Gooding ME, Liao HX, Le PT, Haynes BF. T cell receptor excision circle assessment of thymopoiesis in aging mice. *Mol Immunol*. 2002;38(11):841-848.
14. Callicott RJ, Womack JE. Real-time PCR assay for measurement of mouse telomeres. *Comp Med*. 2006;56(1):17-22.
15. Cawthon RM. Telomere measurement by quantitative PCR. *Nucleic Acids Res*. 2002;30(10):e47.
16. Norddahl GL, Wahlestedt M, Gisler S, Sigvardsson M, Bryder D. Reduced repression of cytokine signaling ameliorates age-induced decline in hematopoietic stem cell function. *Aging Cell*. 2012;11(6):1128-1131.
17. Irizarry RA, Hobbs B, Collin F, et al. Exploration, normalization, and summaries of high density oligonucleotide array probe level data. *Biostatistics*. 2003;4(2):249-264.
18. Li C, Hung Wong W. Model-based analysis of oligonucleotide arrays: model validation, design issues and standard error application. *Genome Biol*. 2001;2(8):RESEARCH0032.
19. Rossi DJ, Jamieson CH, Weissman IL. Stems cells and the pathways to aging and cancer. *Cell*. 2008;132(4):681-696.

20. Allsopp RC, Cheshier S, Weissman IL. Telomere shortening accompanies increased cell cycle activity during serial transplantation of hematopoietic stem cells. *J Exp Med*. 2001;193(8):917-924.
21. Subramanian A, Tamayo P, Mootha VK, et al. Gene set enrichment analysis: a knowledge-based approach for interpreting genome-wide expression profiles. *Proc Natl Acad Sci U S A*. 2005;102(43):15545-15550.
22. Gonzalez B, Denzel S, Mack B, Conrad M, Gires O. EpCAM is involved in maintenance of the murine embryonic stem cell phenotype. *Stem Cells*. 2009;27(8):1782-1791.
23. Flores I, Blasco MA. The role of telomeres and telomerase in stem cell aging. *FEBS Lett*. 2010;584(17):3826-3830.
24. Marion RM, Strati K, Li H, et al. Telomeres acquire embryonic stem cell characteristics in induced pluripotent stem cells. *Cell stem cell*. 2009;4(2):141-154.
25. Agarwal S, Loh YH, McLoughlin EM, et al. Telomere elongation in induced pluripotent stem cells from dyskeratosis congenita patients. *Nature*. 2010;464(7286):292-296.
26. Beerman I, Bhattacharya D, Zandi S, et al. Functionally distinct hematopoietic stem cells modulate hematopoietic lineage potential during aging by a mechanism of clonal expansion. *Proc Natl Acad Sci U S A*. 2010;107(12):5465-5470.
27. Dykstra B, Olthof S, Schreuder J, Ritsema M, de Haan G. Clonal analysis reveals multiple functional defects of aged murine hematopoietic stem cells. *J Exp Med*. 2011;208(13):2691-2703.
28. Sudo K, Ema H, Morita Y, Nakauchi H. Age-associated characteristics of murine hematopoietic stem cells. *J Exp Med*. 2000;192(9):1273-1280.
29. Kim M, Moon HB, Spangrude GJ. Major age-related changes of mouse hematopoietic stem/progenitor cells. *Ann N Y Acad Sci*. 2003;996:195-208.
30. Chiang YJ, Calado RT, Hathcock KS, Lansdorp PM, Young NS, Hodes RJ. Telomere length is inherited with resetting of the telomere set-point. *Proc Natl Acad Sci U S A*. 2010;107(22):10148-10153.
31. Kim K, Doi A, Wen B, et al. Epigenetic memory in induced pluripotent stem cells. *Nature*. 2010;467(7313):285-290.
32. Lister R, Pelizzola M, Kida YS, et al. Hotspots of aberrant epigenomic reprogramming in human induced pluripotent stem cells. *Nature*. 2011;471(7336):68-73.
33. Polo JM, Liu S, Figueroa ME, et al. Cell type of origin influences the molecular and functional properties of mouse induced pluripotent stem cells. *Nat Biotechnol*. 2010;28(8):848-855.
34. Young MA, Larson DE, Sun CW, et al. Background mutations in parental cells account for most of the genetic heterogeneity of induced pluripotent stem cells. *Cell stem cell*. 2012;10(5):570-582.
35. Welch JS, Ley TJ, Link DC, et al. The origin and evolution of mutations in acute myeloid leukemia. *Cell*. 2012;150(2):264-278.
36. Attema JL, Pronk CJ, Norddahl GL, Nygren JM, Bryder D. Hematopoietic stem cell ageing is uncoupled from p16 INK4A-mediated senescence. *Oncogene*. 2009;28(22):2238-2243.
37. Bracken AP, Kleine-Kohlbrecher D, Dietrich N, et al. The Polycomb group proteins bind throughout the INK4A-ARF locus and are disassociated in senescent cells. *Genes & development*. 2007;21(5):525-530.
38. De Haan G, Gerrits A. Epigenetic control of hematopoietic stem cell aging the case of Ezh2. *Annals of the New York Academy of Sciences*. 2007;1106:233-239.

FIGURE LEGENDS

Figure 1. Transcriptional alterations of HSC aging persist through transplantation-mediated stress. (A) Experimental outline. (B) Venn diagrams depicting the number of genes up- or downregulated in HSCs with age, and the overlap of genes that remain differentially regulated as a consequence of HSC aging following transplantation. Numbers in Venn diagrams depict differentially regulated probe sets, with numbers in brackets indicating unique genes. The identities of common genes are shown below each diagram. The analysis was performed on gene expression arrays from two independent experiments totaling six replicate arrays for the young and aged steady-state setting and two replicate arrays for the young and aged transfer setting. Abbreviations: HSC; Hematopoietic Stem Cell.

Figure 2. Generation of iPS cells from bone marrow hematopoietic progenitor cells. (A) FACS strategy to isolate candidate iPS cells from hematopoietic stem and progenitor cells. HSPCs were transduced with retroviruses expressing *GFP*, *Oct3/4*, *Klf4*, *c-Myc* and *Sox2* for two days and subsequently cultured for 14 days in ES cell conditions. On day 14, candidate iPS cells were isolated by FACS based on a GFP-CD45-EpCAM+SSEA-1+ phenotype and cultured in individual wells (25 cells sorted per well) until single iPS colonies emerged. (B) Representative FACS plots of a commercially available C57BL/6 ES cell line (Primogenix B6N1, LEFT), and an established iPS line showing the simultaneous expression of EpCAM and SSEA-1 (RIGHT). (C) Expression of pluripotency factors and induction of *Nanog* expression in established iPS lines (five independent experiments, 3 replicates / cell line). (D) Correlation plots of the genome-wide expression patterns of Young and Aged BiPS lines to ESCs (one independent experiment, relative expression values were averaged from two replicate arrays per condition). A correlation plot of expression patterns in ESC to HSCs is also shown to highlight the similarity in expression patterns of iPS lines and ESCs. (E) Y chromosome FISH of a cross-section of the hippocampus from a negative control female mouse (TOP) and an Aged^{BiPS} primary chimera (BOTTOM) generated from male Aged^{BiPS} cells injected into a female blastocyst. (F) FACS plots showing the congenic immunophenotype (CD45.1/CD45.2 system) of the hematopoietic cells used for cell isolation and primary chimera

generation. (BOTTOM RIGHT) Peripheral blood phenotype of a germline contributed Aged^{BiPS} offspring. Abbreviations: FACS; Fluorescence-activated Cell Sorting, HSPCs; Hematopoietic Stem and Progenitor Cells, iPS; induced Pluripotent Stem, ESC; Embryonic stem cell, FISH; Fluorescent In Situ Hybridization.

Figure 3. Single-cell telomere length analysis of HSCs from various sources. (A) The relative telomere length was measured by qPCR in single sorted HSCs in two independent experiments from 3 individual young and aged mice, respectively (n=251 and 246 cells in each group). (B) Single cell telomere length measurements of blastocyst- and AgedBiPS2-derived HSCs from an AgedBiPS2 primary chimera (n = 86 and 66 cells in each group respectively). (C) Relative telomere length in blastocyst, AgedBiPS1- and AgedBiPS2-derived HSCs isolated from repopulated recipient mice (two independent isolations, n = 200, 130 and 53 cells respectively). (D) Relative telomere length in (LEFT) blastocyst and AgedBiPS derived HSCs from a germline founder (AgedBiPS2 primary chimera, n = 43 and 41 cells in each group respectively) and (RIGHT) from a germline offspring mouse compared to an age-matched C57BL/6 control (n=84 cells in each group). Error bars indicate mean ± SEM.

Figure 4. Hematopoiesis derived from iPS lines with an aged hematopoietic progenitor origin display multiple young functional characteristics. (A) Ratios of the peripheral lineage distribution in individual chimeric animals derived from young and aged BiPS lines. Chimeric ratios are depicted as described previously [26,27] for both blastocyst derived (B) and iPS derived (i) hematopoiesis. Numbers above bars denote individual mice, whose total blood cell chimerism can be found in Table S2. (B) The frequency of HSCs among lineage negative Sca-1 positive c-kit positive bone marrow cells in steady-state young and aged mice (three independent experiments, 6 and 9 mice respectively), and among blastocyst- and AgedBiPS-derived lineage negative Sca-1 positive c-kit positive bone marrow cells in primary chimeras (three independent experiments, totaling 8, 3, and 5 mice respectively). (C) Competitive repopulating ability of young, aged, AgedBiPS1 and AgedBiPS2 HSCs assessed as the ability of each transplanted HSC to repopulate the peripheral myeloid compartment of lethally irradiated young recipients 16 weeks post transfer (three independent experiments, n = 5, 25, 12 and 25 mice per group respectively). (D) *In vivo* lineage

distribution following transplantation of Young and Aged BiPS HSCs into lethally irradiated young recipients. Analysis was performed as in (A). (E) The ability of transplanted young, aged, blastocyst, AgedBiPS1 and AgedBiPS2 derived HSCs to generate naïve TREC+ T cells in repopulated recipient mice (from two independent experiments, totaling 4, 4, 10, 3 and 7 mice respectively). Bars depict mean ± SEM. Abbreviations: BiPS; Blood induced pluripotent stem, TREC; T cell Receptor Excision Circles.

A

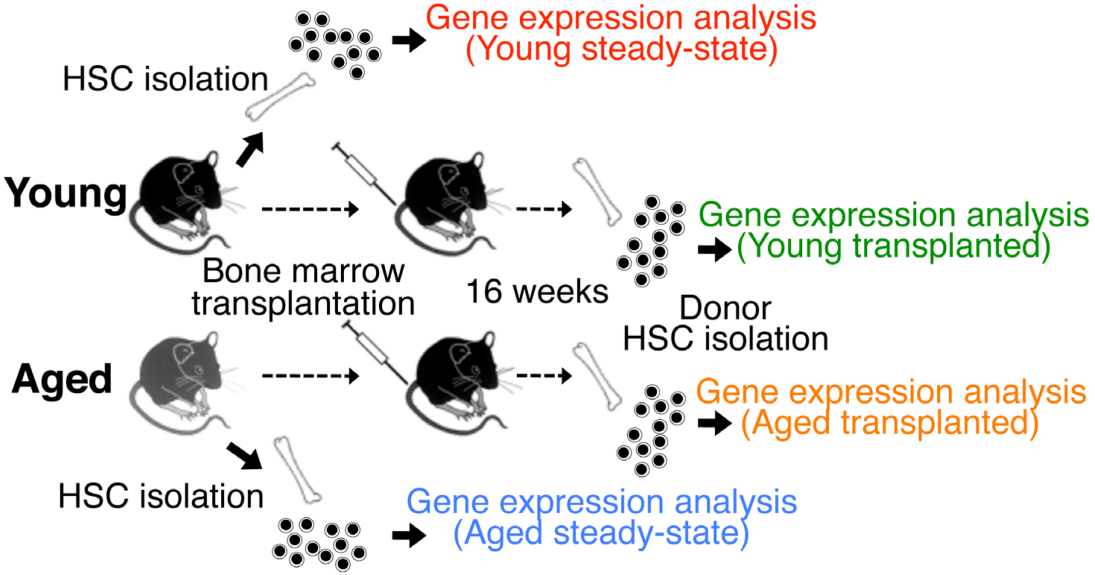

B

Fold over odds: 5.1; p=0.000002

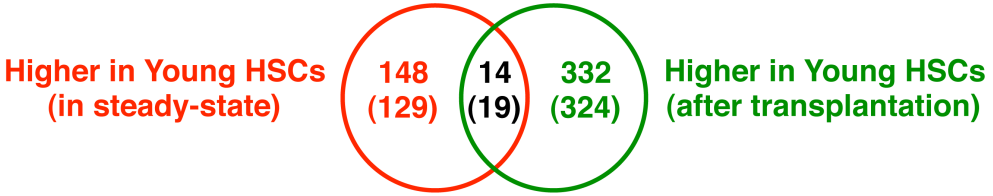

4933439C20Rik, Arhgap30, Baz1b, Cdca5, Cdt1, Efcab7, Gata1, Hmga2, Kif23, Kntc1, LOC433762, LOC63229, Mm.157900.2, Mm.214467.1, Pank1, Plac8, Rad51ap1, Slc22a3, Syk

Fold over odds: 10.7; p<0.000001

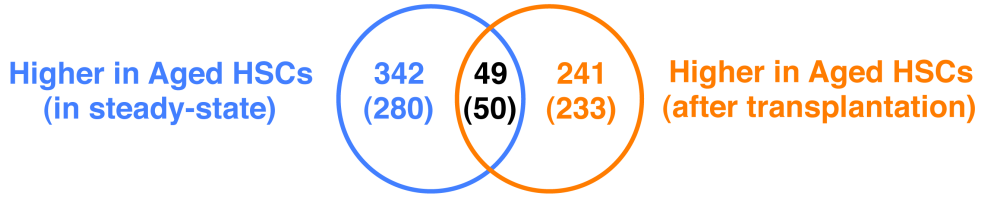

1700112E06Rik, 2310001H12Rik, Alcam, Arhgap6, Bmpr1a, Cd302, Cd38, Clca1/// Clca2, Clca1, Clec1a, Csprs, Cyp26b1, Cysltr2, D14Ertd449e, EG665317, ENSMUSG00000076577, Epas1, Eya4, Fap, Ffar2, Gda, Gem, Itsn1, Jam2, Lamp2, Ldhd, LOC100044677, LOC664787, Mab21l2, Mllt3, Mm.22185.1, Mm.38121.1, Mt2, Nrg4, Nupr1, Obfc2a, P2ry5, Plcl1, Plscr2, Ramp2, Rorb, Sdc4, Sdpr, Selp, Stxbp4, Sult1a1, Tbc1d8, Tm4sf1, Trpc1, Wwtr1

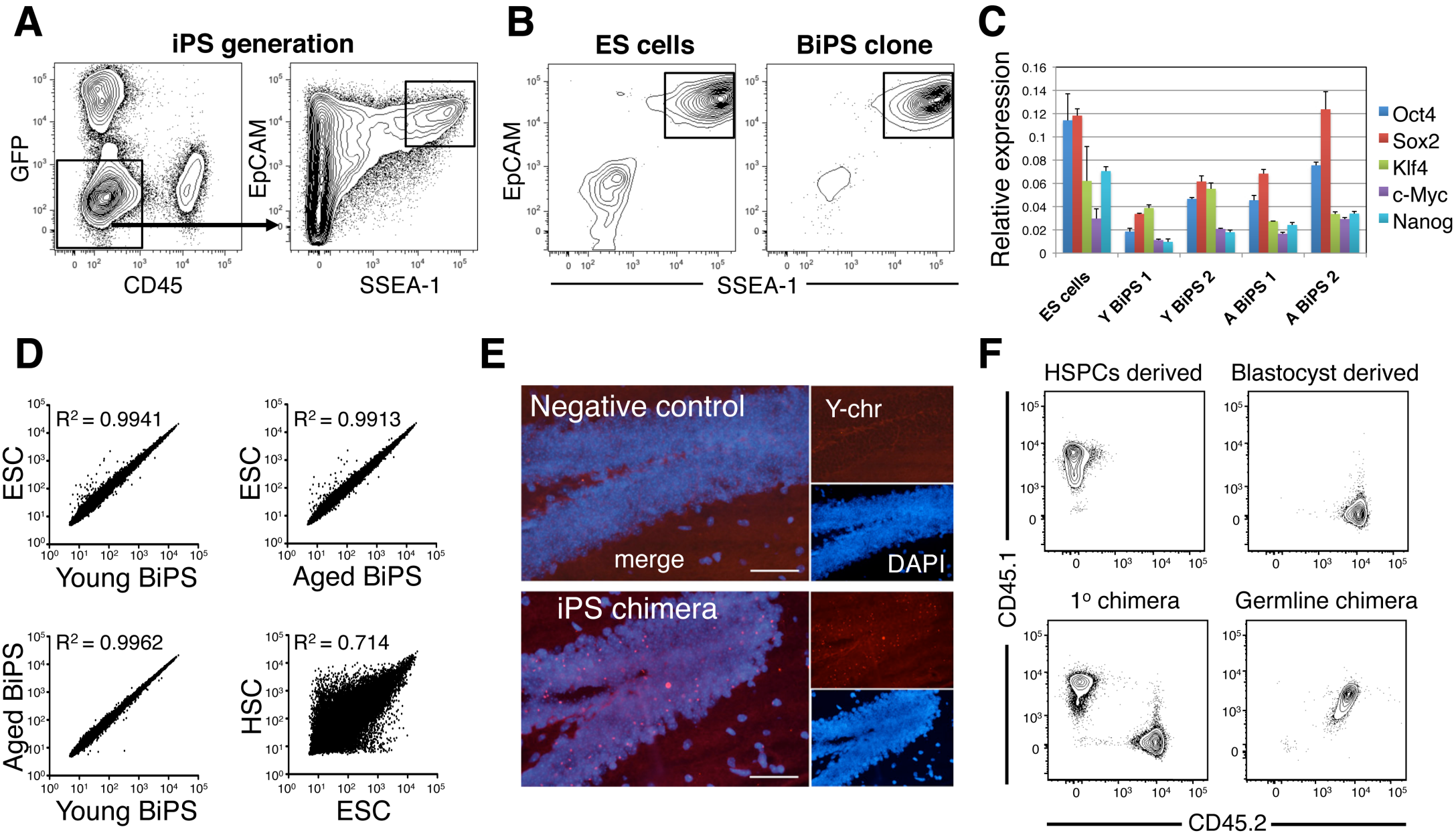
A
iPS generation
GFP
CD45
EpCAM
SSEA-1
B
ES cells
BiPS clone
EpCAM
SSEA-1
C
Relative expression
0.16
0.14
0.12
0.1
0.08
0.06
0.04
0.02
0
Oct4
Sox2
Klf4
c-Myc
Nanog
ES cells
Y BiPS 1
Y BiPS 2
A BiPS 1
A BiPS 2
D
R² = 0.9941
ESC
Young BiPS
R² = 0.9913
ESC
Aged BiPS
R² = 0.9962
Aged BiPS
Young BiPS
R² = 0.714
HSC
ESC
E
Negative control
Y-chr
merge
DAPI
iPS chimera
F
HSPCs derived
Blastocyst derived
1º chimera
Germline chimera
CD45.1
CD45.2

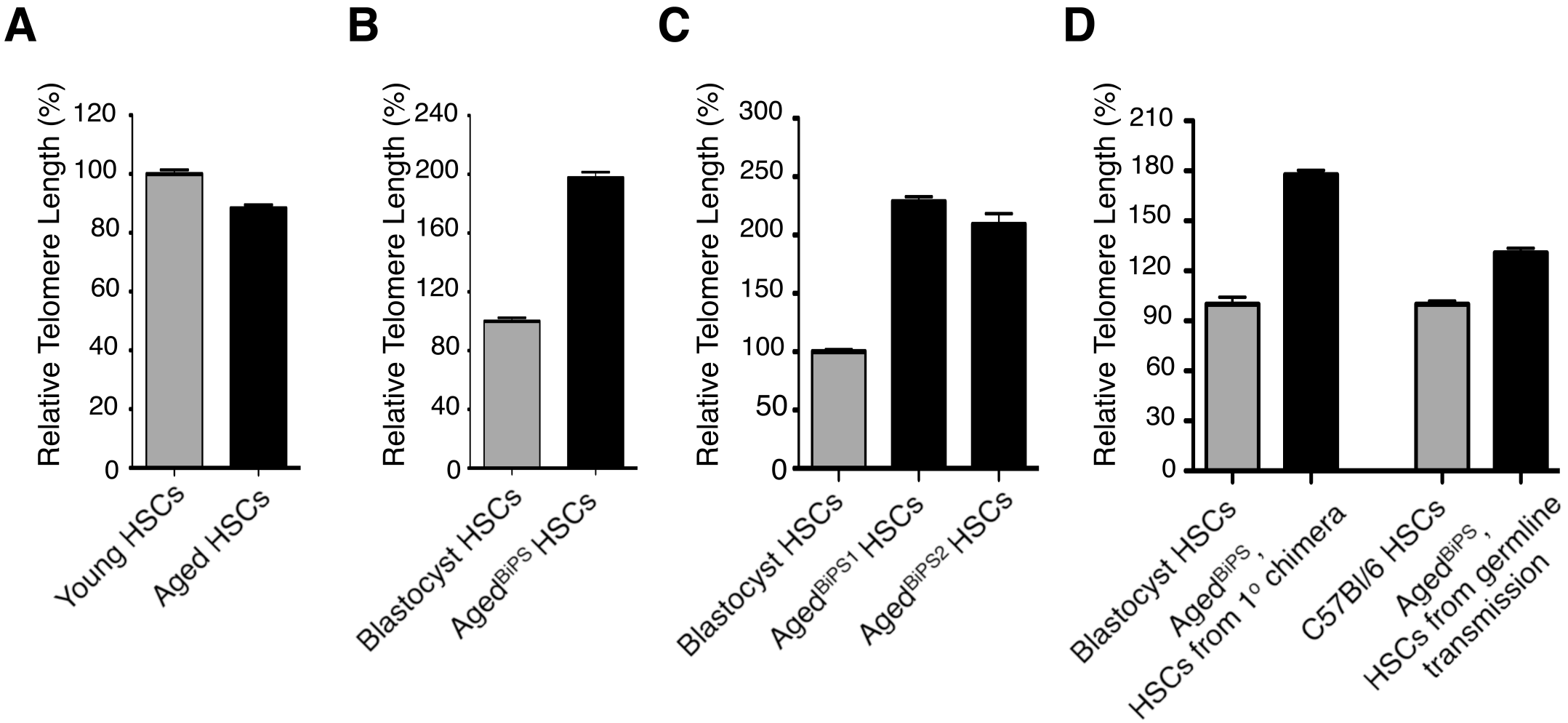
A
Relative Telomere Length (%)
120
100
80
60
40
20
0
Young HSCs
Aged HSCs
B
Relative Telomere Length (%)
240
200
160
120
80
40
0
Blastocyst HSCs
Aged BiPS HSCs
C
Relative Telomere Length (%)
300
250
200
150
100
50
0
Blastocyst HSCs
Aged BiPS1 HSCs
Aged BiPS2 HSCs
D
Relative Telomere Length (%)
210
180
150
120
90
60
30
0
Blastocyst HSCs
Aged BiPS, HSCs from 1° chimera
C57Bl/6 HSCs
Aged BiPS, HSCs from germline transmission

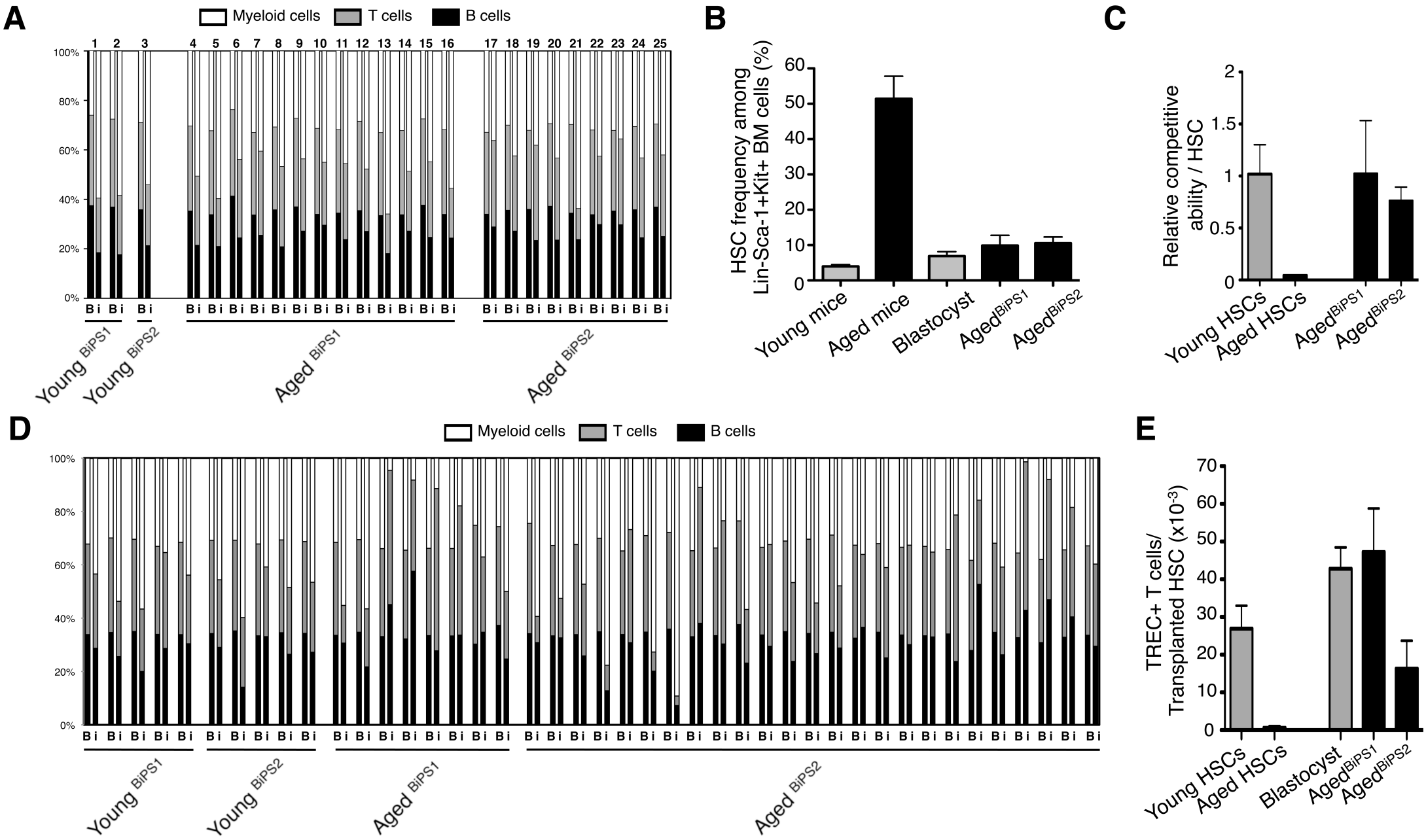
A
Myeloid cells
T cells
B cells
100%
80%
60%
40%
20%
0%
Young BiPS1
Young BiPS2
Aged BiPS1
Aged BiPS2
B
HSC frequency among Lin-Sca-1+Kit+ BM cells (%)
Young mice
Aged mice
Blastocyst
AgedBiPS1
AgedBiPS2
C
Relative competitive ability / HSC
Young HSCs
Aged HSCs
AgedBiPS1
AgedBiPS2
D
Myeloid cells
T cells
B cells
Young BiPS1
Young BiPS2
Aged BiPS1
Aged BiPS2
E
TREC+ T cells/ Transplanted HSC (x10-3)
Young HSCs
Aged HSCs
Blastocyst
AgedBiPS1
AgedBiPS2

SUPPLEMENTARY DATA

The supplemental material accompanying this study consists of a figure showing a GSEA analysis of young and aged steady-state and transplanted HSCs, a figure depicting expression levels of the identified age-associated differentially expressed genes in this study with that of two other datasets, a movie showing contracting cardiomyocytes, an excel spreadsheet with probe sets used in gene expression analyses and a table summarizing generated BiPS chimeric mice.

SUPPLEMENTAL DATA LEGENDS

Figure S1: GSEA of genes differentially regulated as a consequence of aging in steady state, and compared to the gene expression patterns of young and aged HSCs subjected to transplantation. The reciprocal analyses are also shown. The analysis was performed on gene expression arrays from two independent experiments totaling six replicate arrays for the young and aged steady-state setting and two replicate arrays for the young and aged transfer setting. Abbreviations: GSEA; Gene Set Enrichment Analysis.

Figure S2. Correlation of the genes identified to be differentially expressed in young and aged steady-state and transplanted HSCs to two publicly available datasets. Shown are bar charts depicting the expression levels of the differentially expressed coinciding with both steady-state and transplanted HSCs as a function of age in steady-state Dataset 1[1] and Dataset 2[2]. "NA" indicates the absence of probe sets for the analyzed transcripts in Dataset 1. Expression levels are shown relative to the levels in young HSCs of each dataset. Bars depict mean ± SEM.

Movie S1. Movie showing contracting cardiomyocytes *in vitro* differentiated from $Aged^{BiPS}$.

Table S1. Excel spreadsheet containing differentially expressed genes upon steady-state aging and after transplantation of young and aged HSCs.

Table S2. Summary of blastocyst injection experiments and blood chimerism levels in chimeric mice generated using Young and Aged BiPS cells. Chimeras #1-25 correspond to #1-25 in Fig. 4A.

REFERENCES

1. Chambers SM, Shaw CA, Gatza C, Fisk CJ, Donehower LA, Goodell MA. Aging hematopoietic stem cells decline in function and exhibit epigenetic dysregulation. *PLoS biology*. 2007;5(8):e201.
2. Rossi DJ, Bryder D, Zahn JM, et al. Cell intrinsic alterations underlie hematopoietic stem cell aging. *Proceedings of the National Academy of Sciences of the United States of America*. 2005;102(26):9194-9199.

SUPPLEMENTAL TABLES

TABLE S2

Donor line	**Blastocysts injected**	**Pups (% of implanted)**	**Chimeras (% of pups)**	**Blood cell chimerism**
Young^{BiPS1}	19	9 (47.4%)	2 (22.2%)	Chimera #1: 13.6% Chimera #2: 15.7%
Young^{BiPS2}	28	3 (10.7%)	1 (33.3%)	Chimera #3: 14.3%
Total, Young clones	***47***	***12 (25.5%)***	***3 (25%)***	***14.5% (13.6% - 15.7%)***
Aged^{BiPS1}	70	40 (57.1%)	13 (32.5%)	Chimera #4: 13.0% Chimera #5: 3.2% Chimera #6: 48.4% Chimera #7: 4.8% Chimera #8: 14.3% Chimera #9: 35.5% Chimera #10: 14.1% Chimera #11: 9.8% Chimera #12: 23.1% Chimera #13: 13.0% Chimera #14: 6.6% Chimera #15: 29.6% Chimera #16: 5.4%
Aged^{BiPS2}	46	22 (47.8%)	9 (40.1%)	Chimera #17: 14.2% Chimera #18: 26.1% Chimera #19: 21.6% Chimera #20: 28.3% Chimera #21: 7.0% Chimera #22: 12.7% Chimera #23: 36.0% Chimera #24: 20.7% Chimera #25: 28.4%
Total, Aged clones	***116***	***62 (53.4%)***	***22 (33.9%)***	***18.9% (3.2%-48.4%)***

SUPPLEMENTAL FIGURES

FIGURE S1

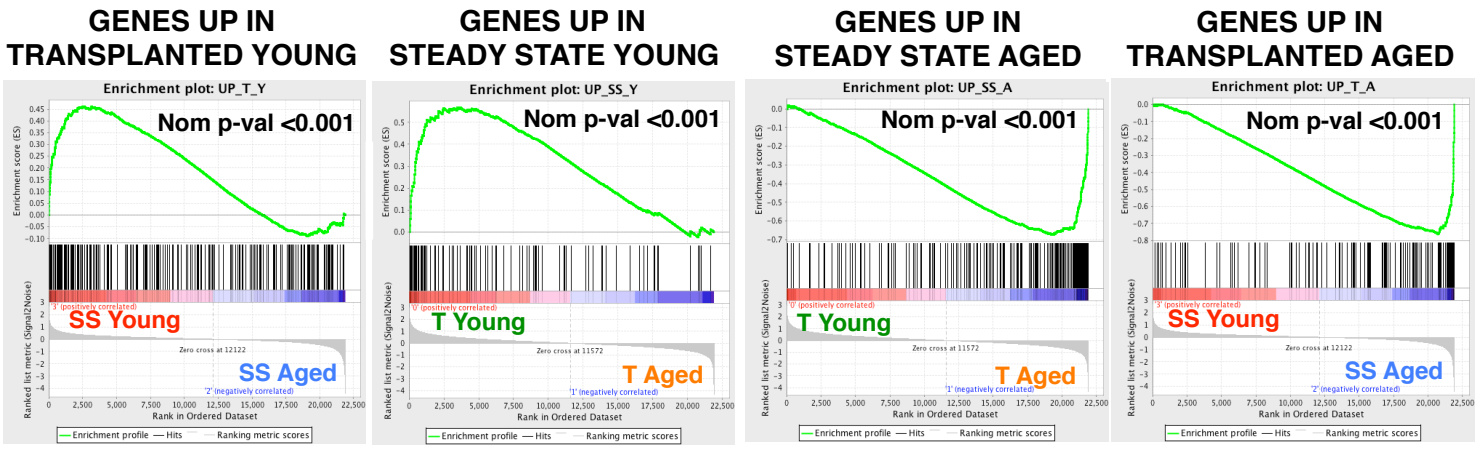

FIGURE S2


A
4933439C20Rik
Arhgap30
Bzrb
Cdca5
Cdt1
Efcab7
Gata1
Hmga2
Kif23
Kntc1
LOC433762
LOC63229
Mm.157900.2
Mm.214467.1
Pank1
Plac8
Rad51ap1
Slc22a3
Syk
B
1700112E06Rik
2310001H12Rik
Alcam
Arhgap6
Bmpr1a
Cd302
CD38
Clca1//Clca2
Clca1
Clec1a
Csprs
Cyp26b1
Cysltr2
D14Ertd449e
EG665317
ENSMUSG00000076577
Epas1
Eya4
Fap
Ffar2
Gda
Gem
Itsn1
Jam2
Lamp2
Ldhd
LOC100044677
LOC664787
Mab21l2
Mll3
Mm.22185.1
Mm.38121.1
Mt2
Nrg4
Nupr1
Obfc2a
P2ry5
Plcl1
Plscr2
Ramp2
Rorb
Sdc4
Sdpr
Selp
Stxbp4
Sult1a1
Tbc1d8
Tm4sf1
Trpc1
Wwtr1
Expression relative to young HSCs
Dataset 1 - Young
Dataset 1 - Aged
Dataset 2 - Young
Dataset 2 - Aged
NA NA